# Preclinical Evaluation of a Tailor-Made DOTA-Conjugated PSMA Inhibitor with Optimized Linker Moiety for Imaging and Endoradiotherapy of Prostate Cancer

Martina Benešová[1], Martin Schäfer[1], Ulrike Bauder-Wüst[1], Ali Afshar-Oromieh[2], Clemens Kratochwil[2], Walter Mier[2], Uwe Haberkorn[2,3], Klaus Kopka[1], and Matthias Eder[1]

*[1]Division of Radiopharmaceutical Chemistry, German Cancer Research Center (DKFZ), Heidelberg, Germany; [2]Department of Nuclear Medicine, University Hospital Heidelberg, Heidelberg, Germany; and [3]Clinical Cooperation Unit Nuclear Medicine, German Cancer Research Center (DKFZ), Heidelberg, Germany*

Despite many advances in the past years, the treatment of metastatic prostate cancer still remains challenging. In recent years, prostate-specific membrane antigen (PSMA) inhibitors were intensively studied to develop low-molecular-weight ligands for imaging prostate cancer lesions by PET or SPECT. However, the endoradiotherapeutic use of these compounds requires optimization with regard to the radionuclide-chelating agent and the linker moiety between chelator and pharmacophore, which influence the overall pharmacokinetic properties of the resulting radioligand. In an effort to realize both detection and optimal treatment of prostate cancer, a tailor-made novel naphthyl-containing DOTA-conjugated PSMA inhibitor has been developed. **Methods:** The peptidomimetic structure was synthesized by solid-phase peptide chemistry and characterized using reversed-phase high-performance liquid chromatography and matrix-assisted laser desorption/ionization mass spectrometry. Subsequent $^{67/68}$Ga and $^{177}$Lu labeling resulted in radiochemical yields of greater than 97% or greater than 99%, respectively. Competitive binding and internalization experiments were performed using the PSMA-positive LNCaP cell line. The in vivo biodistribution and dynamic small-animal PET imaging studies were investigated in BALB/c *nu/nu* mice bearing LNCaP xenografts. **Results:** The chemically modified PSMA inhibitor PSMA-617 demonstrated high radiolytic stability for at least 72 h. A high inhibition potency (equilibrium dissociation constant [$K_i$] = 2.34 ± 2.94 nM on LNCaP; $K_i$ = 0.37 ± 0.21 nM enzymatically determined) and highly efficient internalization into LNCaP cells were demonstrated. The small-animal PET measurements showed high tumor-to-background contrasts as early as 1 h after injection. Organ distribution revealed specific uptake in LNCaP tumors and in the kidneys 1 h after injection. With regard to therapeutic use, the compound exhibited a rapid clearance from the kidneys from 113.3 ± 24.4 at 1 h to 2.13 ± 1.36 percentage injected dose per gram at 24 h. The favorable pharmacokinetics of the molecule led to tumor-to-background ratios of 1,058 (tumor to blood) and 529 (tumor to muscle), respectively, 24 h after injection. **Conclusion:** The tailor-made DOTA-conjugated PSMA inhibitor PSMA-617 presented here is sustainably refined and advanced with respect to its tumor-targeting and pharmacokinetic properties by systematic chemical modification of the linker region. Therefore, this radiotracer is suitable for a first-in-human theranostic application and may help to improve the clinical management of prostate cancer in the future.

Received Aug. 21, 2014; revision accepted Feb. 25, 2015.

For correspondence or reprints contact: Matthias Eder, German Cancer Research Center (DKFZ), Im Neuenheimer Feld 280, 69120 Heidelberg, Germany.
E-mail: m.eder@dkfz-heidelberg.de

Published online Apr. 16, 2015.

COPYRIGHT © 2015 by the Society of Nuclear Medicine and Molecular Imaging, Inc.

**Key Words:** prostate cancer; PSMA; theranostic radiopharmaceuticals; PET imaging; endoradiotherapy

**J Nucl Med 2015; 56:914–920**
DOI: 10.2967/jnumed.114.147413

In western societies, prostate cancer (PCa) continues to be the most common cancer in elderly men and the third most frequent cause of cancer-related mortality (*1*). Consequently, there is a high clinical demand for more effective treatment options in the case of metastatic and hormone-refractory PCa. Specific cancer targeting based on low-molecular-weight radioligands may offer a more accurate and rapid visualization, improved staging, and highly effective endoradiotherapy.

On the basis of small molecules, promising PET radiotracers have been investigated in the last couple of years for the imaging of PCa such as $^{18}$F-fluoro- or $^{11}$C-choline (*2,3*), $^{18}$F-fluoro- or $^{11}$C-acetate, $^{11}$C-methionine, and peptidyl radiotracers based on the gastrin-releasing peptide receptor and the prostate-specific membrane antigen (PSMA) (*4–6*).

Because PSMA is strongly expressed in PCa and upregulated in poorly differentiated, metastatic, and hormone-refractory carcinomas (*7,8*), it represents a highly attractive target in nuclear medicine, potentially meeting the clinical requirements for an effective therapy of metastatic PCa. In particular, urea-based peptidomimetic inhibitors of PSMA were investigated mainly for diagnosis and shown to image advantageously PSMA-expressing PCa (*9–11*). Because of low expression levels in healthy tissue, however, PSMA has additionally the potential for high-dose endoradiotherapy, with minimized radioactivity-related side effects.

An in vivo theranostic approach combines the potential of both diagnosis and therapy in one and the same targeting molecule by labeling with either a diagnostic or a suitable therapeutic radionuclide. The β emitters such as $^{90}$Y, $^{131}$I, and $^{177}$Lu are appropriate candidates for current systemic radionuclide therapy. Both $^{131}$I and $^{177}$Lu emit γ radiation in addition to its $\beta^-$ particle, whereas $^{90}$Y is a pure $\beta^-$ emitter (*12*). Recently, the promising therapeutic low-molecular-weight compound $^{131}$I-MIP-1095 was clinically investigated. In this study, 28 men with metastatic castration-resistant PCa were treated with $^{131}$I-MIP-1095 (mean injected activity, 4.8 GBq). The treatment has shown a significant impact on the tumor lesions and prostate-specific antigen (PSA) values and resulted in



Patent Owner Exhibit 2078
IPR2025-01582

a reduction of bone pain. However, because of the high fraction of γ radiation, patients were obliged to stay in the hospital for around 1 wk. In addition, mild hematologic toxicities were observed (*13*). Endoradiotherapy with the aforementioned radiometals, however, bear a high potential to improve the clinical situation. For example, $^{177}$Lu presents a lower proportion of γ radiation, which would result in a reduced stay in the hospital and lower hemotoxicity in comparison to $^{131}$I (*12*).

Thus, a novel theranostic compound was designed consisting of 3 components: the pharmacophore glutamate-urea-lysine; the chelator DOTA, able to complex both $^{68}$Ga and $^{177}$Lu; and a linker connecting these 2 entities. The linker turned out to be crucial for high imaging contrasts (*14*) because the chemical structure determines the internalization potency of the PSMA inhibitors (*15*). Besides the targeting properties, modifications of the linker might also influence the pharmacokinetic properties of peptidomimetic PSMA inhibitors and, therefore, improve their therapeutic potential (*16*). This study presents the preclinical evaluation of a tailor-made linker-optimized theranostic PSMA inhibitor with considerably optimized pharmacokinetic and targeting properties. Finally, the first individual clinical diagnostic experience with this novel radiotracer is shown, underlining its clinical potential.

## MATERIALS AND METHODS

All chemicals, reagents, and solvents for the synthesis and analysis of the compound were analytic grade (for radiosynthesis ultrapure and metal-free); purchased from Sigma Aldrich, Merck, Iris Biotech, or CheMatech; and used without further purification.

The synthesis of PSMA-617 is summarized in Figure 1. The peptidomimetic glutamate-urea-lysine binding motif (steps 1–6) and the linker were synthesized by solid-phase peptide chemistry as previously described (*17*).

The conjugation of the chelator was performed using DOTA-tris(tBu)ester (the supplemental materials provide detailed synthesis information; supplemental materials are available at http://jnm.snmjournals.org). The final product (PSMA-617) was cleaved from the resin and deprotected.

The compound (~42% yield) was analyzed and purified by reversed-phase high-performance liquid chromatography (RP-HPLC) and matrix-assisted laser desorption/ionization mass spectrometry (MALDI-MS) (the supplemental materials provide detailed method information).

$^{68}$Ga (half-life [$T_{1/2}$], 68 min; maximum energy of positrons [$\beta^+$], 1.9 MeV [88%]) was gained from a $^{68}$Ge/$^{68}$Ga generator based on a pyrogallol resin support (*18*) as [$^{68}$Ga]$GaCl_3$ in 0.1 M HCl. $^{67}$Ga ($T_{1/2}$, 3.26 d; energy of photons [γ]/roentgen radiation [x], 94 keV [40%], 184 keV [24%], 296 keV [22%]) was purchased from MDS Nordion as [$^{67}$Ga]$GaCl_3$ in 0.1 M HCl. $^{177}$Lu ($T_{1/2}$, 6.71 d; maximum energy of electrons [$\beta^-$], 497 keV [79%]; energy of photons [γ]/roentgen radiation [x], 113 keV [6%], 208 keV [11%]) was obtained from PerkinElmer as [$^{177}$Lu]$LuCl_3$ in 0.05 M HCl.

Typically, 80–95 μL of 2.4 M HEPES (4-(2-hydroxyethyl)-1-piperazineethanesulfonic acid; pH 7.5) were mixed with 20 μL of [$^{68}$Ga]$Ga^{3+}$ eluate (~70 MBq) or 5 μL of [$^{67}$Ga]$GaCl_3$ (~50 MBq) and adjusted to pH 4.0 with 10%–30% NaOH or 0.1 M HCl, respectively. Subsequently, 5 μL of 0.1–1 mM PSMA-617 (0.5–5 nmol) in 0.1 M HEPES were added. The reaction mixture was incubated at 95°C for 15 min. Radiolabeling was performed without any separation of labeled and nonlabeled compound. The specific activity for [$^{68}$Ga]PSMA-617 was in the range of 14–140 GBq/μmol and for [$^{67}$Ga]PSMA-617 in the range of 10–100 GBq/μmol. For $^{177}$Lu labeling, 112 μL of sodium acetate (0.4 M; pH 5.0), 5 μL of [$^{177}$Lu]$LuCl_3$ (~20 MBq), and 5 μL of 0.1–1 mM PSMA-617 (0.5–5 nmol) in 0.1 M HEPES were mixed and incubated for 20 min at 95°C. The specific activity was in the range of 4–40 GBq/μmol. The radiochemical yield was determined by analytic RP-HPLC and reversed-phase thin-layer chromatography (RP-TLC) on silica gel plates (60 RP-18$F_{254S}$; Merck) with 0.1 M sodium citrate as a mobile phase.

The radiochemical stability of $^{67/68}$Ga-labeled PSMA-617 in phosphate-buffered saline (PBS) and human serum up to 72 h at 37°C was tested by RP-TLC. The lipophilicity was determined via the distribution of $^{67/68}$Ga-labeled PSMA-617 in the 2-phase system n-octanol and HEPES buffer. The serum protein binding was analyzed by gel filtration (the supplemental materials provide detailed method information).

Both in vitro and in vivo experiments were performed using the PSMA-positive LNCaP cell line (androgen-sensitive human lymph node metastatic lesion of prostatic adenocarcinoma, CRL-1740 [American Type Culture Collection]). The cells were supplemented with 10% fetal calf serum and L-glutamine and incubated at 37°C in an environment of humidified air containing 5% $CO_2$. For in vivo

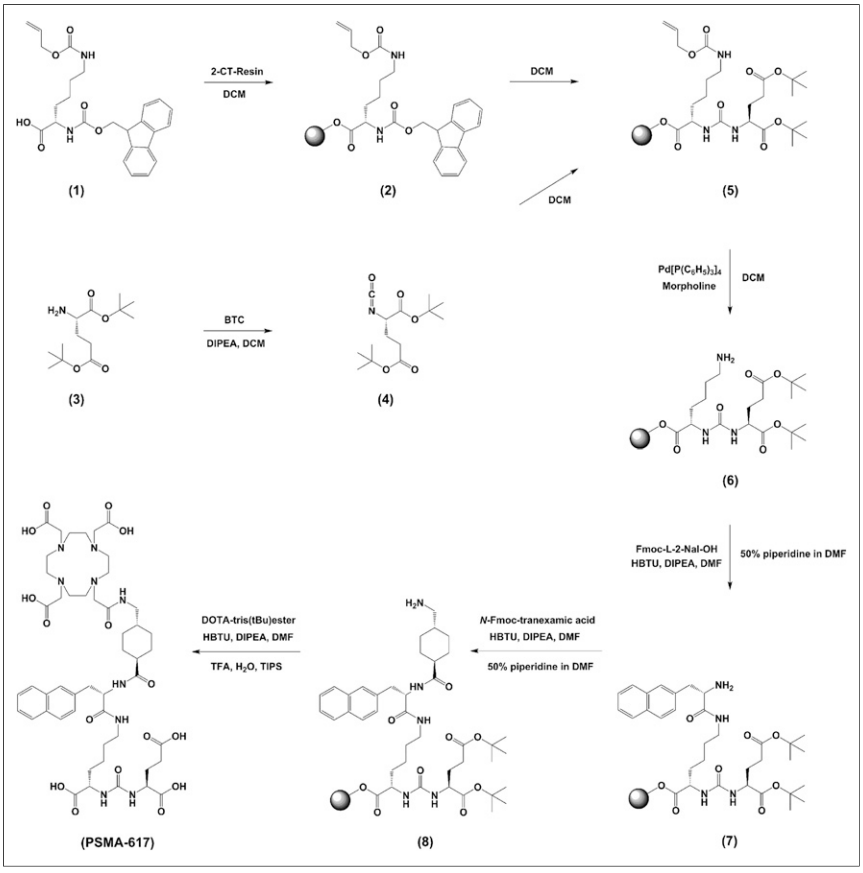


**FIGURE 1.** Synthesis of DOTA-conjugated PSMA inhibitor PSMA-617.

**TABLE 1**
Analytic Data of Compound PSMA-617

| Compound | Molecular weight (g/mol) | Retention time (min) of… Nonlabeled ligand on analytic HPLC | [$^{67/68}$Ga]Ga-PSMA-617 | [$^{177}$Lu]Lu-PSMA-617 | m/z* | logD n-octanol/HEPES |
|---|---|---|---|---|---|---|
| PSMA-617 | 1,042.15 | 2.63 | 2.97 | 3.06 | 1,043.3 | −2.00 |

*Mass spectrometry of nonlabeled ligand detected as $[M+H]^+$.

experiments, 8-wk-old BALB/c *nu/nu* mice were subcutaneously inoculated into the right trunk with $5 \times 10^6$ LNCaP cells in 50% Matrigel (Discovery Labware). When the size of the tumor was approximately 1 $cm^3$, the radiolabeled compound was injected via the tail vein (~30 MBq, 0.5 nmol for small-animal PET imaging; ~1 MBq, 0.06 nmol for organ distribution).

The binding affinity of PSMA-617 was assayed by enzyme-based (NAALADase) and cell-based competitive assays. Data obtained from both experiments were fitted using a nonlinear regression algorithm (GraphPad Prism 5; GraphPad Software) to obtain the 50% inhibitory concentration.

The NAALADase assay is based on a competitive reaction of recombinant human PSMA (R&D Systems) with nonlabeled PSMA-617 and was performed as previously described (*17*) (the supplemental materials provide detailed method information).

Meanwhile, PSMA-617 became commercially available (CAS no. 9933, PSMA-617; ABX Advanced Biochemical Compounds, chemical characteristics were proved to be identical) and was additionally used as radioligand in the internalization assay. The assay was performed as described previously (*19*) (the supplemental materials provide detailed method information).

For small-animal PET imaging with $^{68}$Ga-labeled PSMA-617, a 50-min dynamic scan and a static scan from 100 to 120 min after injection were obtained (the supplemental materials provide detailed method information).

For organ distribution, the animals were sacrificed after indicated time points (from 1 to 24 h). The distributed radioactivity ($^{67/68}$Ga or $^{177}$Lu, respectively) was measured in all dissected organs and in blood using a $\gamma$ counter. The values are expressed as percentage injected dose per gram (%ID/g).

The first clinical diagnostic study with [$^{68}$Ga]Ga-PSMA-617 PET/CT (1 h after injection) was performed as previously published (*20–22*). The administered mass of [$^{68}$Ga]Ga-PSMA-617 was 2 $\mu$g. The administered activity was 288 MBq. There were no adverse or other clinically detectable pharmacologic effects. No significant changes in vital signs were observed. The outcome from this study will be described in more detail in a further publication.

## RESULTS

The chemical analysis is summarized in Table 1. PSMA-617 was stable for at least 6 mo as a lyophilized fluffy white powder and also in a solution of dimethylsulfoxid-*d6* or hexadeuterodimethyl sulfoxide, respectively, both at −20°C, as shown by RP-HPLC and MALDI-MS. A precursor amount of 0.5 nmol was labeled with radiogallium, with a radiochemical yield of greater than 90% in 15 min at 95°C, for both $^{67}$Ga or $^{68}$Ga. Small-animal PET imaging was performed after purification by means of solid-phase extraction using SepPak C18 cartridges (Waters). A higher amount of precursor (5 nmol) resulted in a radiochemical yield of greater than 97%. Radiolabeling with $^{177}$Lu gained a radiochemical yield of greater than 99% at low amounts of precursor (0.5 $\mu$g, 0.5 nmol).

For determination of the radiolytic stability, PSMA-617 was radiolabeled with $^{68}$Ga or $^{67}$Ga and incubated at 37°C for 1 or 24 h, respectively, both in PBS and in human serum. [$^{68}$Ga]Ga-PSMA-617 showed a high stability after 1 h in PBS and in human serum, respectively, as indicated by TLC. After 24 h, values demonstrated 1% of free activity in PBS and less than 4% in human serum. Long-term stability with $^{177}$Lu did not reveal any free activity after 1 and 24 h, neither in PBS nor in serum. After 48 h, less than 0.4% and after 72 h less than 0.6% of free $^{177}$Lu was measured in serum and less than 0.2% and less than 0.6% in PBS, respectively. The stability of the compound was also confirmed via gel filtration with a Sephadex column (Merck). This run did not demonstrate any transfer of activity to human serum proteins after 1 h of incubation at 37°C.

PSMA-617 revealed nanomolar affinity for PSMA on LNCaP cells (equilibrium dissociation constant $[K_i] = 2.34 \pm 2.94$ nM; $n = 7$). In addition, the inhibition potency was determined for the $^{nat}$Ga- and $^{nat}$Lu-labeled PSMA-617. No significant difference in

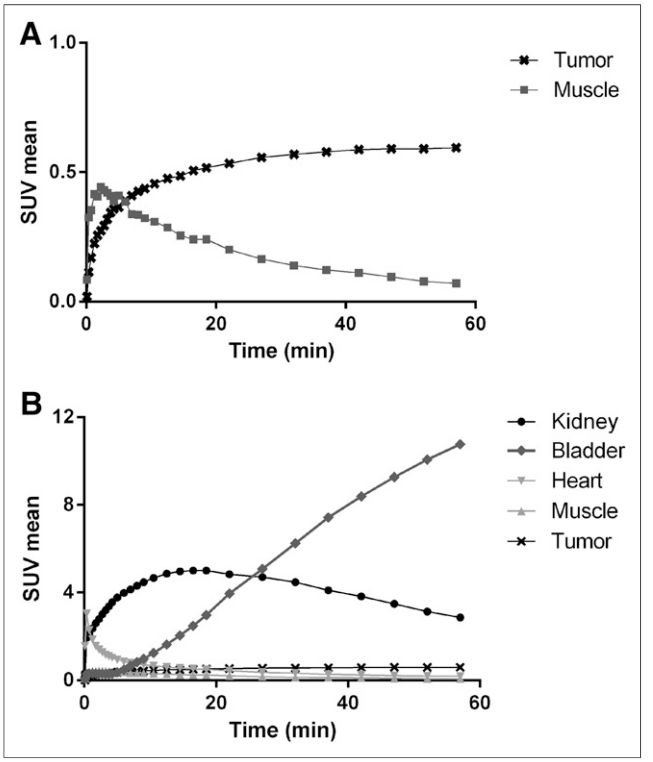


**FIGURE 2.** Time–activity-curves for tumor and background (A) and for relevant organs (B) up to 1 h after injection of 0.5 nmol of $^{68}$Ga-labeled PSMA-617. Data are mean standardized uptake value (SUVmean).

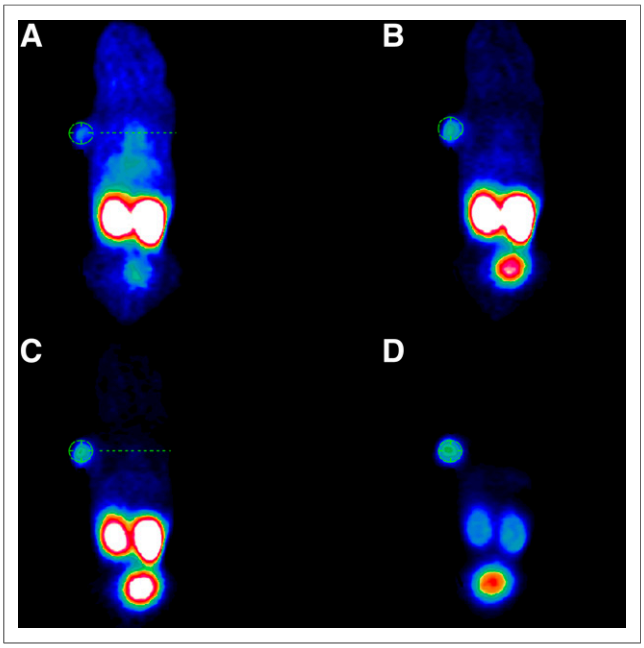


**FIGURE 3.** Whole-body coronal slices from small-animal PET imaging of athymic male nude mouse bearing LNCaP tumor xenografts. Tumor-targeting efficacy and pharmacokinetic properties were evaluated by injection of 0.5 nmol of $^{68}$Ga-labeled PSMA-617 (~30 MBq) with following scans at 0–20 min (A), 20–40 min (B), 40–60 min (C), and 120 min (D) after injection.

binding affinity was observed ($K_i$ = 6.40 ± 1.02 nM for $^{nat}$Ga complex; $K_i$ = 6.91 ± 1.32 nM for $^{nat}$Lu complex). The binding affinity determined by the enzyme-based NAALADase assay was subnanomolar ($K_i$ = 0.37 ± 0.21 nM; $n$ = 2). $^{68}$Ga-labeled PSMA-617 was specifically internalized up to 17.67 ± 4.34 percentage injected activity/$10^6$ LNCaP cells ($n$ = 3) and $^{177}$Lu-labeled PSMA-617 up to 17.51 ± 3.99 percentage injected activity/$10^6$ LNCaP cells ($n$ = 3), both at 37°C.

The time–activity curves obtained from dynamic PET showed a high tumor-to-muscle ratio (8.5) at 1 h after injection (Fig. 2A) and fast clearance from the kidneys, followed by a rapid accumulation of radioactivity in the bladder (Fig. 2B).

The small-animal PET slices (Fig. 3) reveal an increasing tumor uptake up to 2 h after injection and a rapid elimination of radioactivity from other organs, muscles, and blood. The rapid kidney excretion is also demonstrated by the maximum-intensity-projection scans (Fig. 4), whereby tumor uptake is maintained (Fig. 2).

Organ distribution with $^{68}$Ga-labeled PSMA-617 after 1 h ($n$ = 3; Fig. 5A) revealed a high specific uptake in LNCaP tumors (8.47 ± 4.09 %ID/g; 0.98 ± 0.32 %ID/g by coinjection of 2-PMPA) and in the kidneys (113.3 ± 24.4 %ID/g). The high uptake in the kidneys was nearly completely blocked (2.38 ± 1.40 %ID/g) by coinjection of 2 mg of 2-PMPA per kilogram. Other organs such as the liver (1.17 ± 0.10 %ID/g), lung (1.41 ± 0.41 %ID/g), and spleen (2.13 ± 0.16 %ID/g) showed rather low uptake and no blocking effect (data not shown), with the exception of the spleen (0.52 ± 0.36 %ID/g). Tumor-to-background ratios were 7.8 (tumor to blood) and 17.1 (tumor to muscle) at 1 h after injection.

As compared with the $^{68}$Ga-labeled version, the organ distribution with $^{177}$Lu-labeled PSMA-617 ($n$ = 3; Fig. 5B) showed a similar uptake in the LNCaP tumors (11.20 ± 4.17 %ID/g; 0.64 ± 0.07 %ID/g by coinjection of 2-PMPA) and in the kidneys (137.2 ± 77.8 %ID/g; 0.85 ± 0.22 %ID/g by coinjection of 2-PMPA [2 mg/kg]). The uptake of radioactivity in the lung (0.78 ± 0.17 %ID/g; not significant; $P$ = 0.06) and spleen (2.98 ± 1.32 %ID/g; not significant; $P$ = 0.25) demonstrated values similar to $^{68}$Ga-labeled PSMA-617. The liver uptake was found to be statistically different (0.22 ± 0.08 %ID/g; $P < 0.01$). Tumor-to-background ratios determined 1 h after injection showed slightly higher values (tumor to blood, 22.1; tumor to muscle, 25.6) than previous organ distribution with $^{68}$Ga-labeled PSMA-617.

Organ distribution with [$^{177}$Lu]Lu-PSMA-617 ($n$ = 3; Fig. 5C) showed that the high initial kidney uptake was almost completely cleared (2.13 ± 1.36 %ID/g) within 24 h whereas the tumor uptake remained high or even tended to slightly increase (10.58 ± 4.50 %ID/g; not significant; $P$ = 0.55). Other organs such as the liver (0.08 ± 0.03 %ID/g), lung (0.11 ± 0.13 %ID/g), and spleen (0.13 ± 0.05 %ID/g) demonstrated low uptake at 24 h after injection. The favorable pharmacokinetics led to very high tumor-to-background ratios (tumor to blood, 1,058; tumor to muscle, 529) at 24 h after injection.

A side-by-side comparison of [$^{68}$Ga/$^{177}$Lu]Ga/Lu-PSMA-617 ($^{177}$Lu for 24-h biodistribution) with the [$^{67/68}$Ga]Ga-HBED-CC–conjugated (HBED-CC is *N*,*N*′-bis[2-hydroxy-5-(carboxyethyl) benzyl]ethylenediamine-*N*,*N*′-diacetic acid) PSMA inhibitor PSMA-11 ($^{67}$Ga for 24-h biodistribution) (*17*) is presented in Tables 2 and 3 and in Figure 6. Major differences were observed in the spleen (2.13 ± 0.16 and 17.88 ± 2.87 %ID/g; $P < 0.01$), the kidneys (2.13 ± 1.36 and 187.4 ± 25.3 %ID/g; $P < 0.01$), and the tumor (10.58 ± 4.50 and 3.20 ± 2.89 %ID/g; $P$ = 0.07) at 24 h after injection. As compared with 1 h after injection, the kidney uptake of [$^{67}$Ga]Ga-PSMA-11 was not significantly reduced at 24 h after injection whereas [$^{177}$Lu]Lu-PSMA-617 was nearly completely cleared.

Figure 7 shows the encouraging first introductory human [$^{68}$Ga]Ga-PSMA-617 PET/CT imaging of a patient with a PSA level of 20 ng/mL presenting with multiple abdominal metastases.

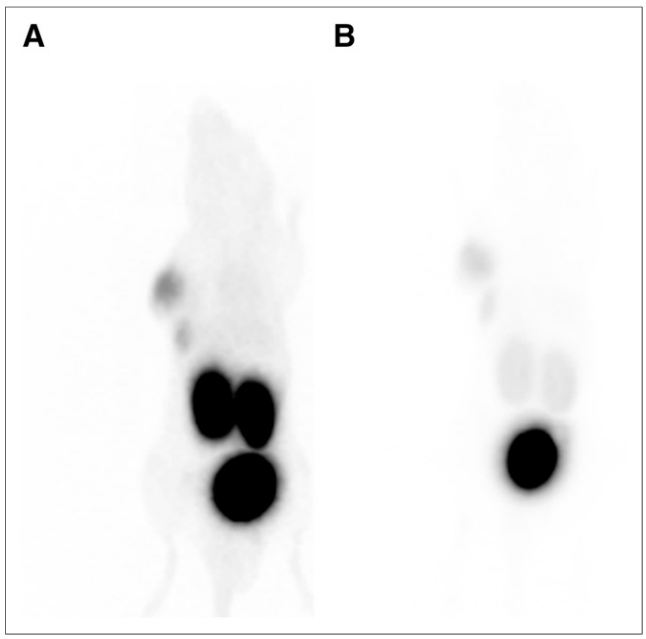


**FIGURE 4.** Whole-body coronal scans as maximum-intensity projections at 60 (A) and 120 min (B) after injection of $^{68}$Ga-labeled PSMA-617.

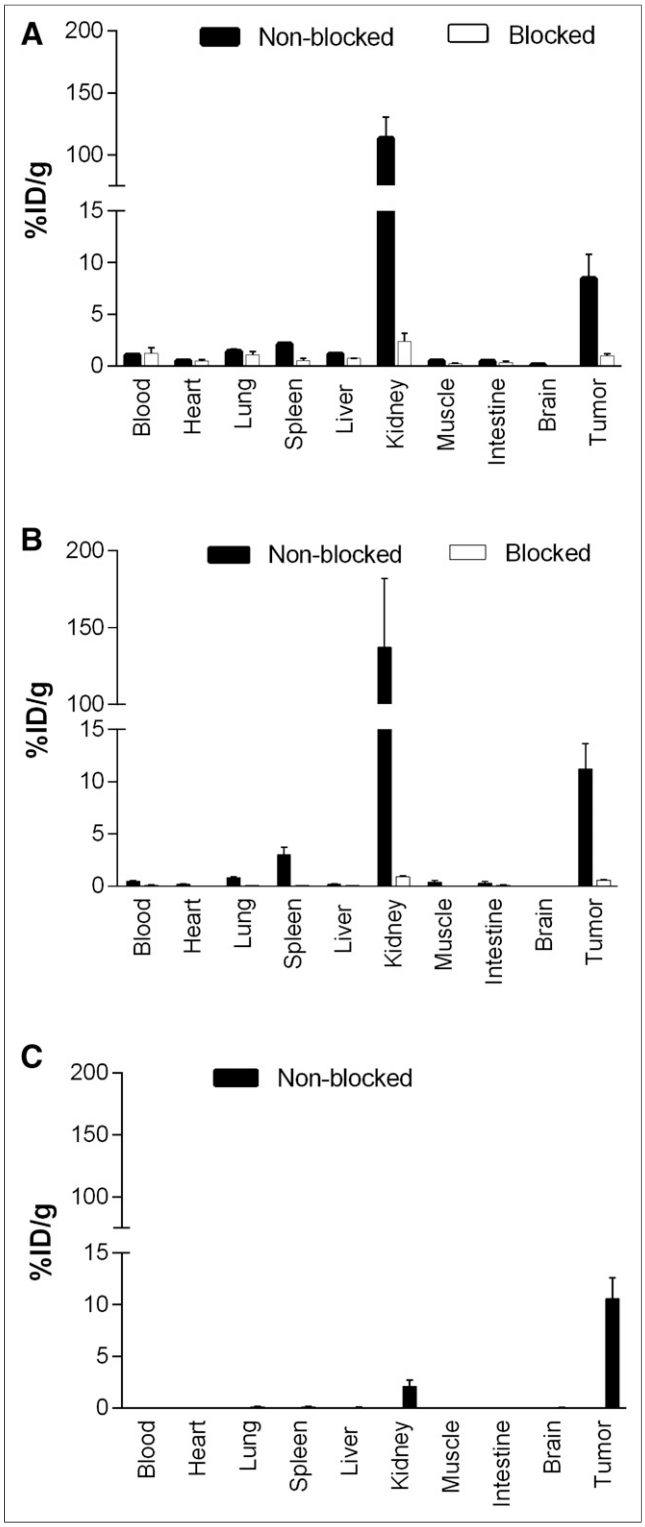


**FIGURE 5.** Organ distribution of 0.06 nmol of [$^{68}$Ga]Ga-PSMA-617 at 1 h after injection (A) and 0.06 nmol of [$^{177}$Lu]Lu-PSMA-617 at 1 (B) and 24 h after injection (C). Specificity was demonstrated by coinjection of 2 mg of 2-PMPA per kilogram of body weight. Uptake in murine kidneys and in tumor proved to be PSMA-specific. Data are %ID/g of tissue ± SD ($n$ = 3).

The lesions were clearly visualized with high tumor uptake and high tumor-to-background ratios already 1 h after intravenous injection.

**TABLE 2**
PSMA Inhibition Potency ($K_i$) of $^{68}$Ga-Labeled PSMA-617 and PSMA-11

| Compound | $K_i$ (nM) |
|---|---|
| [$^{68}$Ga]Ga-PSMA-11 | 12.0 ± 2.8 |
| [$^{68}$Ga]Ga-PSMA-617 | 2.34 ± 2.94 |

Data are mean ± SD ($n$ = 3 for PSMA-11; $n$ = 7 for PSMA-617).

## DISCUSSION

Once a metastatic PCa becomes hormone-refractory there are only a few therapy options, with rather poor clinical success, left. According to the current medical guidelines, antimitotic chemotherapy with docetaxel is typically recommended. However, the overall benefit for the patient is typically poor because of the reported side effects and rather short time to progression, with a reported improvement in overall survival of less than 2.5 mo (*23*).

As a consequence, there is a high clinical demand for more effective—that is, targeted—systemic therapy strategies. Targeted endoradiotherapy offers the possibility to treat the lesions in a specific and tumor-selective manner by addressing cell surface receptors mainly expressed on malignant cells. Because PSMA is highly expressed on the surface of metastatic and hormone-refractory PCa cells and—besides the kidneys and salivary glands—nearly no expression in healthy tissue is found, a highly effective treatment can be expected using radiolabeled urea-based small-molecule inhibitors of PSMA. Besides many encouraging reports about the diagnostic clinical use of urea-based PSMA inhibitors, Zechmann et al. have recently shown promising therapeutic effects with $^{131}$I-labeled MIP-1095 in patients with hormone-refractory PCa. The radiotracer has shown significant lesion uptake in all patients. The PSA values decreased in 60.7% of men treated by more than 50%, and 84.6% of men with bone pain showed complete or moderate reduction of pain (*13*).

Despite these highly encouraging preliminary clinical results, further developments are necessary to optimize the effectivity of treatment and to minimize the reported side effects. The combination of the commonly used chelating agent DOTA with the PSMA-targeting inhibitors opens the possibility of using the same vector molecule for imaging and therapeutic purposes as DOTA effectively forms complexes with diagnostic ($^{68}$Ga) and therapeutic radiometals ($^{90}$Y or $^{177}$Lu). The half-life of $^{68}$Ga matches the pharmacokinetics of low-molecular-weight molecules

**TABLE 3**
Cell Surface Binding and Internalization of PSMA-617 and PSMA-11

| Compound | Cell surface (%IA/10$^6$ cells) | Lysate (%IA/10$^6$ cells) |
|---|---|---|
| [$^{68}$Ga]Ga-PSMA-11 | 10.63 ± 2.93 | 9.47 ± 2.56 |
| [$^{68}$Ga]Ga-PSMA-617 | 14.81 ± 8.67 | 17.67 ± 4.34 |

%IA = percentage injected activity.
Data are mean ± SD ($n$ = 3).

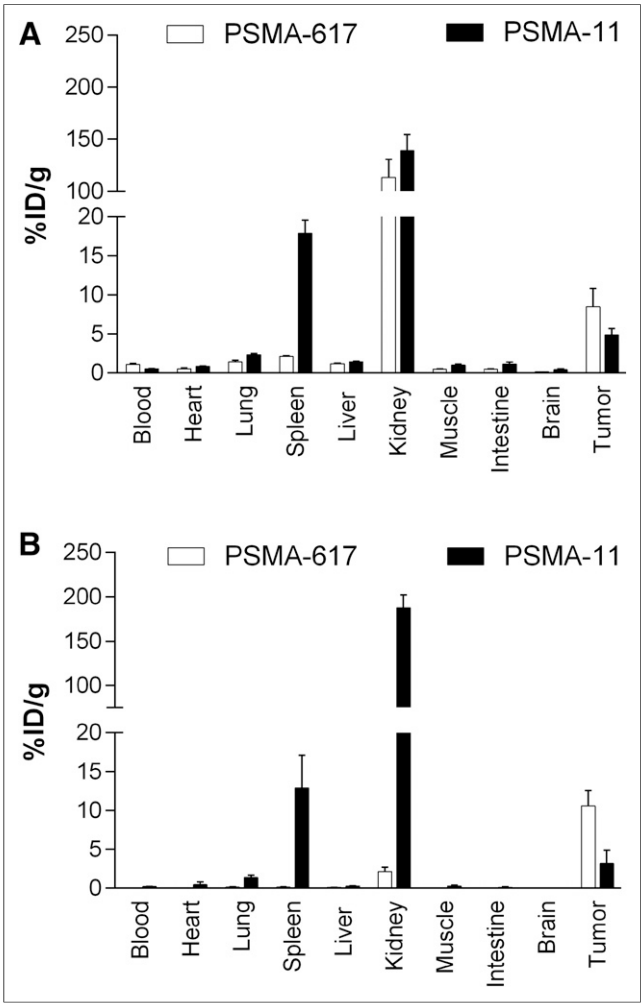


**FIGURE 6.** Organ distribution expressed as %ID/g of tissue ± SD ($n$ = 3) of 0.06 nmol of [$^{68}$Ga]Ga-PSMA-617 and [$^{68}$Ga]Ga-PSMA-11 at 1 h after injection (A) and [$^{177}$Lu]Lu-PSMA-617 and [$^{67}$Ga]Ga-PSMA-11 at 24 h after injection (B).

with relatively fast diffusion, target localization, and blood clearance (*24*). Therapeutic radionuclides such as $^{177}$Lu allow scintigraphy and subsequent dosimetry with the same compound. In comparison to $^{131}$I, $^{177}$Lu presents a lower proportion of $\gamma$ radiation, resulting in a considerably reduced hospitalization, which goes along with improved radiation protection and lowered hemotoxicity (*25*).

In general, theranostics based on radiometals offer targeted and personalized treatment for the patient while minimizing the damage of healthy tissues. From an economic point of view, in vivo theranostics yield an improved outcome for cancer patients, clinical trials can be designed more effectively and efficiently, and finally, individual costs for cancer treatment will be reduced.

Recently, $^{68}$Ga-labeled Glu-urea-Lys-(Ahx)-HBED-CC ([$^{68}$Ga]Ga-PSMA-11) proved to be a successful tracer for PET imaging of recurrent PCa (*17*). It was reported that the chelator HBED-CC seemed to interact advantageously with the lipophilic part of the PSMA binding pocket (*17,22*). However, because of the high selectivity of the complexing agent HBED-CC for $^{68}$Ga, the radiotracer is not suitable for radiolabeling with therapeutic radiometals such as $^{177}$Lu or $^{90}$Y. The here aimed linker region is designed to elucidate the structure–activity relationships and to mimic the proven additional biologic interactions of HBED-CC with the binding pocket. Thus, an ideal linker length (*26*), polarity (*27*), size, flexibility (*28*), presence of aromatic groups (*26*), or hydrophobic functionality distal to the glutamic acid moiety (*29*) represents an effective strategy to design highly potent PSMA inhibitor–based radiotracers.

On the basis of these considerations, a DOTA conjugate of a PSMA inhibitor with optimized targeting properties has been designed in this study. The resulting [$^{68}$Ga]Ga-PSMA-617 exhibits high binding affinity for PSMA and is effectively internalized. Thus, the biologic properties of the novel tracer were significantly improved in comparison with [$^{68}$Ga]Ga-PSMA-11 (*17*). Moreover, dynamic small-animal PET imaging and organ distribution of [$^{68}$Ga]Ga-PSMA-617 showed an early enrichment in the bladder (6 min after injection), and also the maximum kidney uptake was reached as early as 15 min after injection and diminished substantially already after 20 min, whereas [68Ga]Ga-PSMA-617 was further accumulated and retained in the tumor. The favorable pharmacokinetics led to high tumor-to-background ratios (tumor to blood, 1,058; tumor to muscle, 529) with the $^{177}$Lu-labeled version 24 h after injection. In contrast to the clinical PET tracer [$^{68}$Ga]Ga-PSMA-11 (*21*), the initial high kidney uptake was nearly completely cleared 24 h after injection.

Taken together, the studies of PSMA-617 presented here disclose that the presence of the naphthylic linker has a significant impact on the tumor-targeting and biologic activity as well as on imaging contrast and pharmacokinetics, properties which are crucial for both high imaging quality and efficient targeted endoradiotherapy. With regard to therapeutic use, the high binding affinity and internalization, prolonged tumor uptake, rapid kidney clearance, and high tumor-to-background ratio give clear clinical

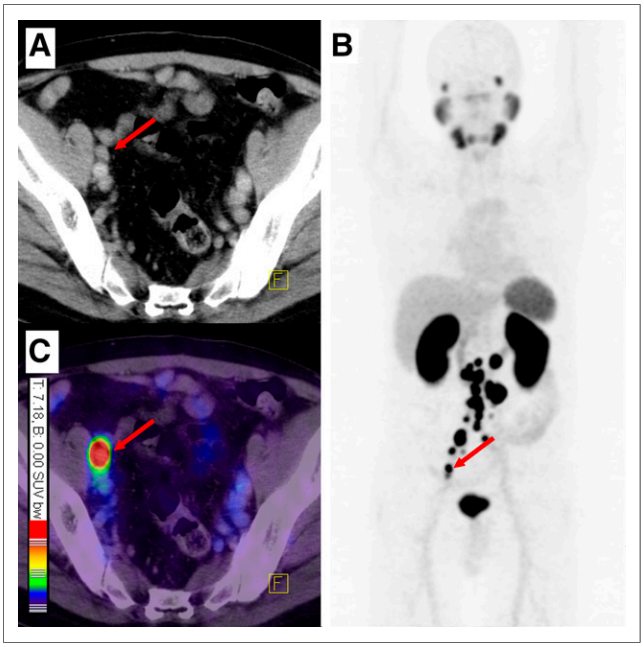


**FIGURE 7.** [$^{68}$Ga]Ga-PSMA-617 PET/CT (1 h after injection) demonstrating a first patient with multiple lymph node metastases. Red arrows point to representative lesion with maximum standardized uptake value (SUV) of 36.5 and a tumor-to-background ratio of 52.1 at 1 h after injection. (A) Contrast-enhanced CT. (B) Maximum-intensity projection of PET scan 1 h after injection. (C) Fusion of PET scan and contrast-enhanced CT.

advantages for PSMA-617, compared with previously published DOTA-based PSMA inhibitors (*11,30*). In comparison to PSMA-11 (*21*), PSMA-617 seems to be more attractive for endoradiotherapy because of its higher tumor uptake at later time points, lower spleen accumulation, and the highly efficient clearance from the kidneys.

The first individual clinical diagnostic experience with $^{68}$Ga-labeled PSMA-617 is comparable with the recently introduced exclusive PET tracer [$^{68}$Ga]Ga-PSMA-11. The fast kidney clearance shown with [$^{177}$Lu]Lu-PSMA-617 encourages us to transfer the compound into the clinical scenario with the aim of a first individual endoradiotherapeutic study. In this connection, a comprehensive first-in-human clinical evaluation of [$^{177}$Lu]Lu-PSMA-617 is under way (*31*).

## CONCLUSION

Theranostic radiotracers provide patients with targeted and personalized treatment options, thereby improving the current clinical treatment options at the same time. The compound PSMA-617 exhibits high PSMA-specific tumor uptake, rapid background clearance, and fast kidney excretion, which gives clear clinical advantages for both high imaging quality and efficient endoradiotherapy of recurrent PCa.

## DISCLOSURE

The costs of publication of this article were defrayed in part by the payment of page charges. Therefore, and solely to indicate this fact, this article is hereby marked "advertisement" in accordance with 18 USC section 1734. This project was supported by a PhD stipend, project no. 101247, provided by the Helmholtz International Graduate School for Cancer Research, a grant from the DFG (Deutsche Forschungsgemeinschaft) (ED234/2-1), and a grant from the Klaus Tschira Foundation. No other potential conflict of interest relevant to this article was reported.

## ACKNOWLEDGMENTS

Animal experiments complied with the current laws of the Federal Republic of Germany. In vivo studies were kindly performed by Ursula Schierbaum and Karin Leotta (both German Cancer Center Research, Heidelberg, Germany).

## REFERENCES

1. Ferlay J, Steliarova-Foucher E, Lortet-Tieulent J, et al. Cancer incidence and mortality patterns in Europe: estimates for 40 countries in 2012. *Eur J Cancer.* 2013;49:1374–1403.
2. Scher B, Seitz M, Albinger W, et al. Value of $^{11}$C-choline PET and PET/CT in patients with suspected prostate cancer. *Eur J Nucl Med Mol Imaging.* 2007;34:45–53.
3. Reske SN, Blumstein NM, Neumaier B, et al. Imaging prostate cancer with $^{11}$C-choline PET/CT. *J Nucl Med.* 2006;47:1249–1254.
4. Jadvar H. Molecular imaging of prostate cancer: PET radiotracers. *AJR.* 2012;199:278–291.
5. Ravizzini G, Turkbey B, Kurdziel K, Choyke PL. New horizons in prostate cancer imaging. *Eur J Radiol.* 2009;70:212–226.
6. Apolo AB, Pandit-Taskar N, Morris MJ. Novel tracers and their development for the imaging of metastatic prostate cancer. *J Nucl Med.* 2008;49:2031–2041.
7. Israeli RS, Powell CT, Corr JG, Fair WR, Heston WD. Expression of the prostate-specific membrane antigen. *Cancer Res.* 1994;54:1807–1811.
8. Israeli RS, Powell CT, Fair WR, Heston WD. Molecular cloning of a complementary DNA encoding a prostate-specific membrane antigen. *Cancer Res.* 1993;53:227–230.
9. Hillier SM, Maresca KP, Femia FJ, et al. Preclinical evaluation of novel glutamate-urea-lysine analogues that target prostate-specific membrane antigen as molecular imaging pharmaceuticals for prostate cancer. *Cancer Res.* 2009;69:6932–6940.
10. Foss CA, Mease RC, Fan H, et al. Radiolabeled small-molecule ligands for prostate-specific membrane antigen: in vivo imaging in experimental models of prostate cancer. *Clin Cancer Res.* 2005;11:4022–4028.
11. Banerjee SR, Pullambhatla M, Byun Y, et al. $^{68}$Ga-labeled inhibitors of prostate-specific membrane antigen (PSMA) for imaging prostate cancer. *J Med Chem.* 2010;53:5333–5341.
12. Kassis AI. Therapeutic radionuclides: biophysical and radiobiologic principles. *Semin Nucl Med.* 2008;38:358–366.
13. Zechmann CM, Afshar-Oromieh A, Armor T, et al. Radiation dosimetry and first therapy results with a $^{124}$I/$^{131}$I labeled small molecule (MIP-1095) targeting PSMA for prostate cancer therapy. *Eur J Nucl Med Mol Imaging.* 2014;41:1280–1292.
14. Wester HJ, Schottelius M, Scheidhauer K, et al. PET imaging of somatostatin receptors: design, synthesis and preclinical evaluation of a novel $^{18}$F-labelled, carbohydrated analogue of octreotide. *Eur J Nucl Med Mol Imaging.* 2003;30:117–122.
15. Liu T, Nedrow-Byers JR, Hopkins MR, Berkman CE. Spacer length effects on in vitro imaging and surface accessibility of fluorescent inhibitors of prostate specific membrane antigen. *Bioorg Med Chem Lett.* 2011;21:7013–7016.
16. Banerjee SR, Foss CA, Castanares M, et al. Synthesis and evaluation of technetium-$^{99m}$- and rhenium- labeled inhibitors of the prostate-specific membrane antigen (PSMA). *J Med Chem.* 2008;51:4504–4517.
17. Eder M, Schäfer M, Bauder-Wüst U, et al. $^{68}$Ga-complex lipophilicity and the targeting property of a urea-based PSMA inhibitor for PET imaging. *Bioconjug Chem.* 2012;23:688–697.
18. Schuhmacher J, Maier-Borst W. A new Ge-68/Ga-68 radioisotope generator system for production of Ga-68 in dilute HCl. *Int J Appl Radiat Isot.* 1981;32:31–36.
19. Schäfer M, Bauder-Wüst U, Leotta K, et al. A dimerized urea-based inhibitor of the prostate-specific membrane antigen for Ga-68-PET imaging. *Eur J Nucl Med Mol Imaging Res.* 2012;2:23–33.
20. Afshar-Oromieh A, Zechmann CM, Malcher A, et al. Comparison of PET imaging with a $^{68}$Ga-labelled PSMA ligand and $^{18}$F-choline based PET/CT for the diagnosis of recurrent prostate cancer. *Eur J Nucl Med Mol Imaging.* 2014;41:11–20.
21. Afshar-Oromieh A, Avtzi E, Giesel FL, et al. The diagnostic value of PET/CT imaging with the $^{68}$Ga-labelled PSMA ligand HBED-CC in the diagnosis of recurrent prostate cancer. *Eur J Nucl Med Mol Imaging.* 2015;42:197–209.
22. Eder M, Neels O, Müller M, et al. Novel preclinical and radiopharmaceutical aspects of [$^{68}$Ga]Ga-PSMA-HBED-CC: a new PET tracer for imaging of prostate cancer. *Pharmaceuticals (Basel).* 2014;7:779–796.
23. Shelley M, Harrison C, Coles B, Stafforth J, Wilt T, Mason M. Chemotherapy for hormone-refractory prostate cancer. *Cochrane Database Syst Rev.* 2006;4:CD005247.
24. Al-Nahhas A, Win Z, Szyszko T, Singh A, Khan S, Rubello D. What can gallium-68 PET add to receptor and molecular imaging? *Eur J Nucl Med Mol Imaging.* 2007;34:1897–1901.
25. de Jong M, Breeman WA, Valkema R, Bernard BF, Krenning EP. Combination radionuclide therapy using $^{177}$Lu- and $^{90}$Y-labeled somatostatin analogs. *J Nucl Med.* 2005;46(suppl 1):13S–17S.
26. Zhang AX, Murelli RP, Barinka C, et al. A remote arene-binding site on prostate specific membrane antigen revealed by antibody-recruiting small molecules. *J Am Chem Soc.* 2010;132:12711–12716.
27. Antunes P, Ginj M, Walter MA, Chen J, Reubi JC, Maecke HR. Influence of different spacers on the biological profile of a DOTA−somatostatin analogue. *Bioconjug Chem.* 2007;18:84–92.
28. Kane RS. Thermodynamics of multivalent interactions: influence of the linker. *Langmuir.* 2010;26:8636–8640.
29. Maung J, Mallari JP, Girtsman TA, et al. Probing for a hydrophobic a binding register in prostate-specific membrane antigen with phenylalkylphosphonamidates. *Bioorg Med Chem.* 2004;12:4969–4979.
30. Behe M, Alt K, Deininger F, et al. In vivo testing of $^{177}$Lu-labelled anti-PSMA antibody as a new radioimmunotherapeutic agent against prostate cancer. *In Vivo.* 2011;25:55–59.
31. Kratochwil C, Giesel FL, Eder M, et al. [$^{177}$Lu]lutetium-labelled PSMA ligand-induced remission in a patient with metastatic prostate cancer. *Eur J Nucl Med Mol Imaging.* 2015;42:987–988.